

## Entrapment of Organic Solutes by the Water Cage in the Nanochannel of MCM-41

Masaharu Okazaki\* and Kazumi Toriyama

*Research Institute of Instrumentation Frontier, National Institute of Advanced Industrial Science and Technology (AIST), 2266-98, Shimoshidami, Moriyama-ku, Nagoya, 463-8560, Japan*

*Received: September 5, 2005; In Final Form: September 29, 2005*

The effect of MCM-41 on the ESR spectrum of an aqueous spin probe solution was observed. The sharp ESR spectrum turns into a rather broad characteristic one leaving a sharper signal as the minor component, immediately after the addition of MCM-41 powder to the system. This observation indicates that MCM-41 traps the solute molecule into the nanochannel by letting the solvent water form a rather stable molecular cage, since the ESR line shape indicates that the nitroxide radical undergoes anisotropic rotation without being adsorbed on the wall. Thermodynamic parameters for this process are estimated from the temperature dependencies of the trapping efficiency. This process is explained in terms of the surface enthalpy of the liquid specifically intensified in the nanospace.

### Introduction

The physicochemical phenomena of liquids in the confined systems have been extensively studied by employing zeolites, silica gel, micelles, and other inhomogeneous systems.<sup>1–4</sup> These are, for example, capillary condensation,<sup>1,2</sup> freezing/melting,<sup>2</sup> liquid–liquid equilibria,<sup>2</sup> molecular dynamics,<sup>1–3</sup> host–guest interaction,<sup>3,4</sup> and chemical reaction.<sup>3,4</sup> The emergence of MCM-41 and its analogues, mesoporous silica (SiO<sub>2</sub>) made by the template method,<sup>5,6</sup> that give regular, stable, and well-defined nanospaces, has accelerated studies on these phenomena in the nanospace<sup>7,8</sup> and resulted in many novel findings. For example, by employing the pulsed field gradient NMR technique, a rapid diffusion has been observed for benzene in the nanochannel of MCM-41 and was interpreted with a model where liquid benzene diffuses through the nanochannel in the gaseous state.<sup>9</sup> 2-Propanol flows through the nanochannel of MCM-41 at an usual pressure employed in chromatography,<sup>10–12</sup> and a photoreaction there is dependent on the magnetic field.<sup>10,11,13</sup> The collective molecular flow, which is a “pseudo-single-file flow”, has been proposed as a model to compromise the rapid flow that is not described by the Poiseuille’s equation and the long pairing time of the two intermediate radicals. The latter is definitely necessary to explain a large magnetic field effect in the reaction.<sup>13–15</sup> These observations suggest the necessity to accumulate experimental data to clarify the structure of the solution systems and their molecular dynamics in the nano dimension.

Here, we focus on the interaction between the solvent water molecules and the organic solutes in the nanochannel of MCM-41. Since molecular processes of aqueous solution in the nano dimension must play important roles in every field of science,<sup>1,16,17</sup> many efforts have been accumulated to clarify the physical properties of water in the nanospaces.<sup>18–20</sup> A great reduction in diffusivity of water molecules has been observed

by both the neutron scattering method<sup>20</sup> and the NMR spin–echo technique.<sup>21</sup> The electron spin resonance (ESR) method was also employed to observe the dynamic structure of the solution system in the micro- and nanospace.<sup>22,23</sup> This method is powerful in characterizing rotational diffusion of free radicals and its anisotropy as well as translational diffusion.<sup>24</sup> In the present study, we observed the effect of MCM-41 on the solute–solvent interaction in the aqueous solutions of a nitroxide radical, which is frequently called as a spin probe, through observing the ESR spectrum. Upon addition of MCM-41 to the system, the spectrum changed drastically into that containing a broad and characteristic signal indicating that the spin probe radical is efficiently trapped in the water cage formed in the nanochannel of MCM-41. The thermodynamic parameters have been estimated, and the process is discussed as the surface phenomenon specifically enlarged in the nanospace. The relation of the present results with some novel phenomena previously found in the solution systems in the nanochannel, e.g., collective molecular diffusion,<sup>10–12</sup> is discussed.

### Experimental Section

MCM-41 was synthesized following the method<sup>25</sup> given in a reference from tetraethyl-*ortho*-silicate and cetyltrimethylammonium bromide. Template molecules are removed by calcination at 820 K for 5 h. The pore size was estimated as 3.4 nm from the lattice constant obtained by the X-ray diffraction (XRD) method, and the surface area obtained by the Brunauer–Emmett–Teller (BET) method. Samples for ESR observation were prepared as follows:<sup>23,26</sup> 30 mg of MCM-41 powder was put into the bottom of the glassware and degassed; 250  $\mu$ L of a nitroxide solution was injected, the vessel was degassed again, and the sample cell was sealed off. The suspension was vigorously mixed, and the ESR observation was made both immediately after mixing and after the sedimentation was completed for the MCM-41 bed. For the sample with no solution left between the MCM-41 particles,<sup>26</sup> the quantity of MCM-41

\* Corresponding author. Telephone: +81-52-7367138. Fax: +81-52-7367224. E-mail address: masa-okazaki@aist.go.jp.

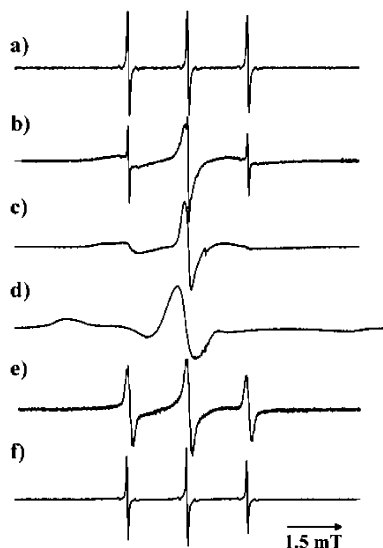
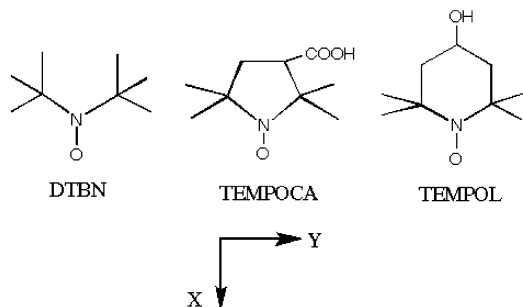


**Figure 1.** ESR spectra for the aqueous solution of DTBN (a–c, f): in the absence of MCM-41 (a), in the MCM-41 bed precipitated from its suspension (b), encapsulated in the MCM-41 nanochannel (c), for a tridecane solution of DTBN in the presence of MCM-41 (d), and for the aqueous solution of TEMPOL in the MCM-41 bed precipitated from its suspension (e). The reference spectrum (f) is observed when Nuculosil-50, a porous silica gel for liquid chromatography, is employed instead of MCM-41. The aqueous solution was not buffered. ESR measurements were made at 298 K.

was increased to 100 mg and the solution volume was reduced to 120  $\mu\text{L}$ . The concentration of the solute was 1.0 mM unless otherwise specified.

The nitroxide radicals were purchased from Aldrich Japan (Tokyo), and other chemicals and high-purity water were from Wako Pure Chemicals (Tokyo, Japan). Nuculosil-50 was purchased from Macherey-Nagel (Germany). ESR measurements were made with a JEOL RX-1 spectrometer (9.1 GHz) with a temperature control unit. The microwave power was set at 1.0 mW, and the modulation amplitude for  $B_0$  was less than that which causes any line distortion. Structures of three nitroxide radicals, di-*t*-butylnitroxide (DTBN), 2,2,5,5-tetramethylpiperidine-1-oxyl-4-ol (TEMPOL), and 2,2,4,4-tetramethylpyrrolidine-3-carboxyl-1-oxyl (TEMPOCA), employed in the present study are shown in Scheme 1 with their molecular coordinates.

#### SCHEME 1



#### Results and Discussion

Figure 1 shows the ESR spectra of nitroxide radicals under various conditions. The sharp three-lined spectrum of aqueous DTBN solution in the absence of MCM-41 (a) indicates that the radical rotates rapidly around every direction. When MCM-41 powder was added to form an aqueous suspension, a broad ESR pattern immediately becomes the major part (b), though

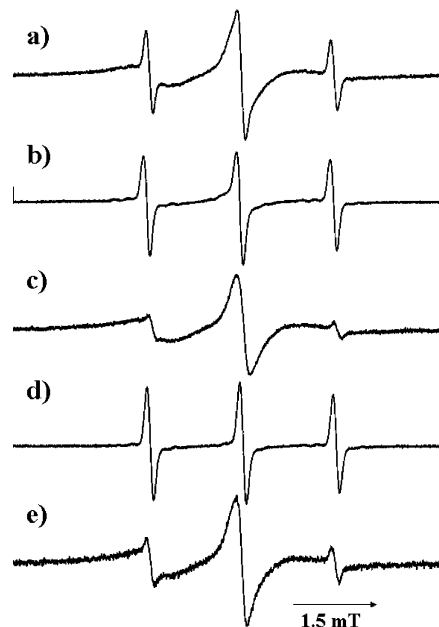


**Figure 2.** ESR spectra of the aqueous TEMPOCA solution (a–c): in the MCM-41 bed precipitated from its suspension, at pH 2.0 (a) and pH 11.0 (b), encapsulated in the MCM-41 nanochannel (c). ESR spectra of TEMPOCA in a mixed solution with water and 2-propanol at the volumetric ratio of 9:1 (d,e): in the MCM-41 bed precipitated from its suspension (d) and encapsulated in the MCM-41 nanochannel (e). The pH was adjusted with the 50 mM phosphate buffers.

the volume of bulk water is nearly equal to or larger than that in the nanochannel. The broad component was selectively observed when the solution between the MCM-41 particles is completely removed from the system (c). We conclude from these observations that the broad and sharp signals correspond to the nitroxide radical in the MCM-41 nanochannel and that in the bulk water phase, respectively. This is the case for every system of the present study and will not be repeated hereafter. The characteristic line shape of the broad component indicates that only the y-axis rotation is allowed considerably in the nanochannel.<sup>26</sup> Therefore, the DTBN molecule must be encapsulated in the rather tight solvent cage formed by the intensified intermolecular network.<sup>26</sup> This spectrum pattern is completely different from the reference spectrum (d) observed for the adsorbed DTBN on the nanochannel, where rotation around all directions is prohibited. The spectrum of TEMPOL in the MCM-41 bed is also constituted of two patterns (e). In this case, however, a considerable part of the TEMPOL radical is left in the bulk phase. This difference may be due to the substituent OH group, which makes the molecule more hydrophilic. A sharp spectrum (f) is observed when Nuculosil-50, a porous silica gel for liquid chromatography, is employed instead of MCM-41, showing that the broad components in spectra (b)–(e) are due to the nitroxide radicals in the nanopore of MCM-41.

Figure 2 shows the ESR spectra for the TEMPOCA systems. In the MCM-41 bed precipitated from the aqueous suspension, the broad component is the main constituent at pH 2.0 (a), which almost disappears at pH 11.0 (b) due to its ionization. The broad component of (a) also disappears when 2-propanol is added at the concentration of 10% (d). When the interparticle water does not exist, the broad component appears again as the main component (c, e) in both the latter cases. The small sharp components in (c, e) may be due to a small amount of solution left outside the nanochannel. The existence of the ionic species used to buffer the pH makes it very difficult to remove all the solution from the bulk space. In the case of DTBN, most of the

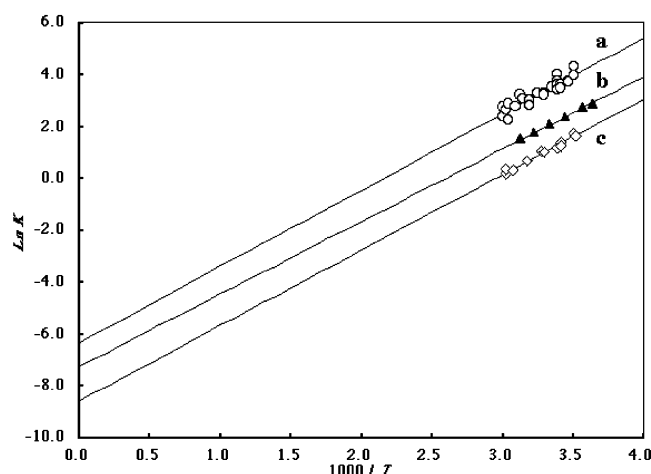
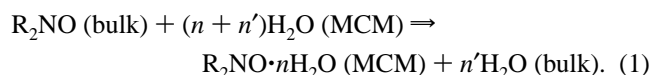


**Figure 3.** Logarithmic plots for the ratios between the concentrations of the nitroxide radicals in the nanochannel and those in the bulk as the functions of  $1000/T$ : a is for DTBN, b for TEMPOCA (pH 2.0), and c for TEMPOL. The relative concentrations were obtained by double integration of their ESR spectra after baseline adjustment.

radicals are trapped in the nanochannel even if 2-propanol is mixed at the concentration of 10% or the pH is brought to 11.0 (spectra not shown). These observations indicate that the driving force for this entrapment is not as strong as in chemisorption, but a rather weak one like that in the hydrophobic interaction in micelle.<sup>27</sup> The micelle core accommodates hydrophobic solutes by liberating the water molecules forming an “iceberg” around the solutes.<sup>27</sup> However, the mechanism of molecular trapping by MCM-41 is different from the typical hydrophobic interaction, since the solute is still surrounded by water molecules in the nanochannel. In fact, the strength of the H-bonding between the NO group of the radical and the water molecules is not altered largely, judging from the  $g$  values<sup>24</sup> of the both components.

The entrapment of solutes in the MCM-41 suspension may proceed as in the following formula:



Here,  $\text{R}_2\text{NO}$ , the nitroxide radical, interacts with  $n$  water molecules as  $\text{R}_2\text{NO} \cdot n\text{H}_2\text{O}$  in the nanochannel. Upon trapping  $\text{R}_2\text{NO}$  as  $\text{R}_2\text{NO} \cdot n\text{H}_2\text{O}$  (MCM), the nanochannel liberates  $n'$   $\text{H}_2\text{O}$  into the bulk. Shown in Figure 3 are the logarithmic plots of the ratio between the quantities of the two components as functions of  $1/T$ , where  $T$  represents the system temperature. The thermodynamic parameters were obtained by using the well-known equation

$$\ln(K) = -\Delta H/RT + \Delta S/R \quad (2)$$

where  $K$  is the ratio between the integrated signal intensities of the broad and sharp components. On the assumption that the thermodynamic activities of water are invariant,  $\Delta H$  and  $\Delta S$  imply the enthalpy and entropy differences, respectively, between the standard states. The results are listed in Table 1.

Although the nitroxide radical is weakly bound in the nanochannel, the absolute values of both  $\Delta H$  and  $\Delta S$  are much larger than those of the freezing process of water, 6.05 kJ/M and 22.1 J/(M·K), respectively. The main part of  $\Delta S$  and  $\Delta H$  must be due to the strengthening of intermolecular H-bonding between the water molecules of  $\text{R}_2\text{NO} \cdot n\text{H}_2\text{O}$  in the MCM-41 nanochannel. Since the enthalpy differences ( $\Delta H$ ) are approximately equal for all the three systems, where the trapping

**TABLE 1: Thermochemical Parameters for the Entrapment of Free Radicals in the Nanochannel of MCM-41<sup>a</sup>**

system	DTBN	TEMPOL	TEMPOCA
$\Delta S$ (J/(M·K))	−52.5	−71.2	−59.3
$\Delta H$ (kJ/M)	−24.4	−24.1	−23.2

<sup>a</sup> The parameters were obtained by the least-squares method.

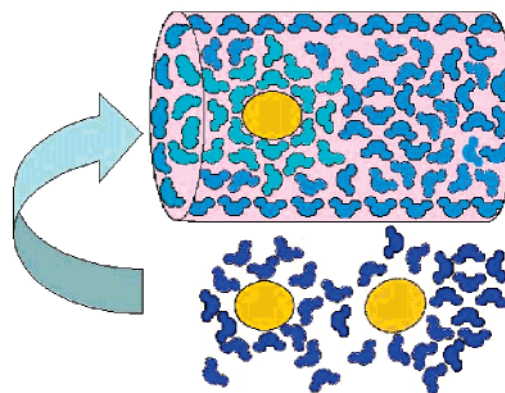


**Figure 4.** A schematic model for the entrapment of a solute molecule by the MCM-41 nanochannel. An apolar molecule (orange) gets into the nanochannel (pink) and is housed in a tight water cage (green) from the bulk water phase, where the housing of the solute with the water molecules (blue) is not steady.

efficiency differs widely, the water cage may not be formed in a flexible way to fit with the solute molecule exactly, and the numbers  $n$  and  $n'$  in eq 1 do not change continuously. The number  $n$  in eq 1 must be larger than 20, because even the dodecahedron cage for the chlorine hydrate is made of 20 water molecules.<sup>28</sup> Since the molecular volume of the solutes is around 10 times as large as that of water, the total number of water molecules associated with the process of eq 1 must be larger than 30. The difference in  $\Delta S$  between the systems may be mainly due to the difference in the number of water molecules that are associated transiently with the solute in the bulk aqueous phase.

It must be fruitful to consider these effects with the usual terms of surface chemistry for the bulk system. The water molecules in a cylinder with radius  $R$  have another enthalpy term  $\Phi = \gamma S$ , where  $\gamma$  is the surface tension and  $S$  is the surface area. This term is rewritten as  $\Phi = 2\gamma(V/R) = N\phi$ , where  $V$  is molar volume and  $N$  is Avogadro's number. So, one molecule at the surface has an additional potential energy of  $\phi = 2\gamma(v/R)$ , on average, where  $v$  is the molecular volume. Since the intermolecular force works to transfer the potential energy inward, molecules are subject to a force field in a nanotube. So, the molecules get some order in this force field, and the physical state may be modified accordingly. For one thing, the water phase in the nanochannel must be less polar; thus, molecules with hydrophobic groups tend to be accommodated there. Once the solute gets into the nanochannel, the water cage is formed in a cooperative manner. This model can also be applied to the other solvent systems. In fact, similar entrapment of nitroxide has been observed for the benzene system, where  $-14.7$  kJ/M and  $-32.5$  J/(M·K) were obtained for  $\Delta H$  and  $\Delta S$ , respectively. The peculiarities of liquids observed so far in the nanochannel, e.g., collective flow of 2-propanol through the nanochannel,<sup>10–12,26</sup> collective diffusion,<sup>23</sup> and phase separation of a solution,<sup>23,26</sup> may also be explained with this model. Since the collective diffusion is a kind of single-file diffusion, most of the PFG-NMR studies on diffusion in the nanospace may be analyzed again by taking this effect into account.

In conclusion, the spin-probe molecules are trapped by a water cage that is made around the solute molecule cooperatively in the nanochannel of MCM-41. The essential picture of the process is drawn as Figure 4, which shows that the solute is trapped in the nanochannel and held in an icy water cage.<sup>29</sup> When the solute goes out from the nanochannel, this icy cage will melt. This trapping mechanism can be explained with the above model taking account of the surface tension on the nanochannel surface, that also explains some peculiarities of liquids in the nanochannel: collective molecular flow and collective diffusion (pseudo-single-file diffusion).

**Acknowledgment.** Financial support of Japan Science and Technology Corp. through the Cooperative System for Supporting Priority Research is acknowledged. This work was partially assisted by a Grant-in-Aid for Scientific Research on Priority Area 'Innovative utilization of strong magnetic fields' (767, 5085208) from MEXT of Japan. Experimental help from Mr. Kohji Fukuzono is also acknowledged.

## References and Notes

- (1) Dullien, F. A. L. In *Porus Media, Fluid Transport and Pore Structure*, 2nd ed.; Academic: New York, 1992.
- (2) Gelb, L. D.; Gubbins, K. E. Radhakrishnan, R.; Sliwubsj-Bartkowiak, M. *Rep. Prog. Phys.* **1999**, *62*, 1573–1659.
- (3) Laeri, F.; Schuth, F.; Simon, U.; Wark, M., Eds. *Host–Guest Systems Based on Nanoporous Crystals*; Wiley-VCH: Weinheim, 2003.
- (4) Nagakura, S.; Hayashi, H.; Azumi, T., Eds. *Dynamic Spin Chemistry*; Kodansha & Wiley: Tokyo and New York, 1998.
- (5) Yanagisawa, T.; Shimizu, T.; Kuroda, K.; Kato, C. *Bull. Chem. Soc. Jpn.* **1990**, *63*, 988–992.
- (6) Kresge, C. T.; Leonowicz, M. E.; Roth, W. J.; Vartuli, J. C.; Beck, J. S. *Nature (London)* **1992**, *359*, 710–712.
- (7) Zhao, X. S.; Lu, G. Q.; Miller, G. J. *Ind. Eng. Chem. Res.* **1996**, *35*, 2075–2090.
- (8) Coma, A. *Chem. Rev.* **1997**, *97*, 2373–2419.
- (9) Stallmach, F.; Graser, A.; Kaerger, J.; Krause, C.; Jeschke, M.; Oberhagemann, U.; Spange, S. *Micropor. Mesopor. Mater.* **2001**, *44–45*, 745.
- (10) Konishi, Y.; Okazaki, M.; Toriyama, K.; Kasai, T. *J. Phys. Chem. B* **2001**, *105*, 9101–9106.
- (11) Okazaki, M.; Toriyama, K.; Oda, K.; Kasai, T. *Phys. Chem. Chem. Phys.* **2002**, *4*, 1201–1205.
- (12) Okazaki, M.; Toriyama, K.; Sawaguchi, N.; Oda, K. *Appl. Magn. Reson.* **2003**, *23*, 435–444.
- (13) Okazaki, M.; Konishi, Y.; Toriyama, K. *Chem. Phys. Lett.* **2000**, *328*, 251–256.
- (14) Okazaki, M.; Sakata, S.; Konaka, R.; Shiga, T. *J. Chem. Phys.* **1987**, *86*, 6792–6800.
- (15) Okazaki, M. In *Dynamic Spin Chemistry*; Nagakura, S., Hayashi, H., Azumi, T., Eds.; Kodansha & Wiley: Tokyo and New York, 1998; Chapter 8.
- (16) Gutfreund, H. In *Enzymes: Physical Principles*; John Wiley: London, 1972.
- (17) Kiricsi, I.; Pal-Borbely, G.; Nagy, J. B.; Karge, H. G. Eds. In *Porous Materials in Environmentally Friendly Processes*; Elsevier: Amsterdam, 1999.
- (18) Dore, J. *Chem. Phys.* **2000**, *258*, 327–347.
- (19) Smirnov, P. I.; Yamaguchi, T.; Kittaka, S.; Takahara, S.; Kuroda, Y. *J. Phys. Chem. B* **2000**, *104*, 5498–5504.
- (20) Takahara, S.; Sumiyama, N.; Kittaka, S. *J. Phys. Chem. B* **2005**, *107*, 11231–11239.
- (21) Hansen, E. W.; Schmidt, R.; Stoeker, M.; Akporiaye, D. *Microporous Mater.* **1995**, *5*, 143–150.
- (22) Martini, G.; Ottaviani, M. F.; Romanelli, M. *J. Colloid Interface Sci.* **1983**, *94*, 105–113.
- (23) Okazaki, M.; Toriyama, K. *J. Phys. Chem. B* **2003**, *107*, 7654–7658.
- (24) Caragheorgheopol, A.; Caldaru, H. EPR Spin-Labeling and Spin-Probe Studies of Self-Assembled Systems. In *Specialist Periodical Reports: Electron Paramagnetic Resonance*; Royal Society of Chemistry: Cambridge, 2000; Vol. 17, pp 205–245.
- (25) Burkett, S. L.; Sims, S. D.; Mann, S. *J. Chem. Soc., Chem. Commun.* **1996**, 1367–1368.
- (26) Okazaki, M.; Toriyama, K. *J. Phys. Chem. B* **2005**, *107*, 13180–13185.
- (27) Fendler, J. H.; Fendler, E. J. In *Catalysis in Micellar and Macromolecular Systems*; Academic: New York, 1975.
- (28) Pauling, L. *The Nature of Chemical Bond*; Cornell University Press: New York, 1960; Chapter 12.
- (29) This water cage must be entitled “iceberg”.